Accounting for prediction error when inferring subsurface fault slip

Z. Duputel, P. S. Agram, R. Jolivet, B. Riel, M. Simons and S. E. Minson

1. Abstract

This study lays the groundwork for a new generation of earthquake source models based on a general formalism that rigorously quantifies the impact of uncertainties in fault slip problems. We distinguish two sources of uncertainty when considering the discrepancy between data and forward model predictions. The first class of error is induced by imperfect measurements and is often referred to as observational error. The second source of uncertainty is generally neglected and corresponds to the prediction error, that is the uncertainty due to imperfect forward modeling. Yet the prediction error can be shown to scale approximately with the size of earthquakes and thus can dwarf the observational error particularly for large events. In this study, we develop physically based statistics for the model prediction error and show how to account for inaccuracies in the Earth model elastic parameters. Of particular importance is the recognition that modeling errors can induce strong spatial and temporal correlations in our observations and that these (co)variances depend the on the amplitude and spatial distribution of fault slip. The advances proposed here are the foundation for a generation of subsurface fault slip models that leads to more reliable images of the earthquake rupture, are more resistant to over-fitting of data and include more realistic estimates of uncertainty on inferred model parameters.

2. On the importance of prediction uncertainty in source inversion problems

2.1 Modeling ingredients

> Data:
- *Field observations*
- *Seismology*
- *Geodesy*
- ...

> Theory:
- *Source geometry*
- *Earth model*
- ...

2.2 Sources of uncertainty

> Observational uncertainty ($\mathbf{C}_d$):
- *Instrumental noise*
- *Ambient seismic noise*

> Prediction uncertainty ($\mathbf{C}_p$): Usually neglected
- *Fault geometry*
- *Earth model*

> For large earthquakes $\mathbf{C}_p >> \mathbf{C}_d$

2.3 A posteriori distribution

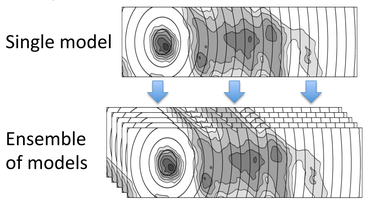

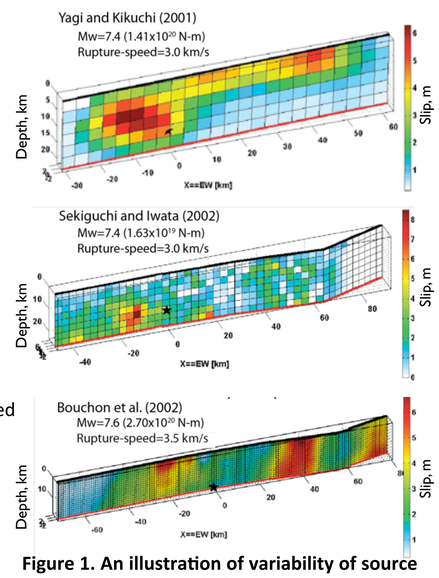

Figure 1. An illustration of variability of source models. Results of finite-source rupture modeling obtained by different research groups are presented for the 1999 Izmit earthquake. The origin of XY coordinates is set at the epicenter location.

3. A realistic statistical model for the prediction uncertainty

3.1 The forward problem

> Solution: $\mathrm{p}(\mathbf{m}|\mathbf{d}_{\mathrm{obs}}) \propto \mathrm{p}(\mathbf{m}) \int_D \mathrm{p}(\mathbf{d}_{\mathrm{obs}}|\mathbf{d})\, \mathrm{p}(\mathbf{d}|\mathbf{m})\, d\mathbf{d}$

Observational error | Prediction uncertainty

Exact theory

$\mathrm{p}(\mathbf{d}|\mathbf{m}) = \delta(\mathbf{d} - \mathrm{g}(\boldsymbol{\mu},\mathbf{m}))$

Stochastic (non-deterministic) theory

$\mathrm{p}(\mathbf{d}|\mathbf{m}) = \mathcal{N}(\mathbf{d} \mid \mathbf{g}(\boldsymbol{\mu},\mathbf{m}), \mathbf{C}_p)$

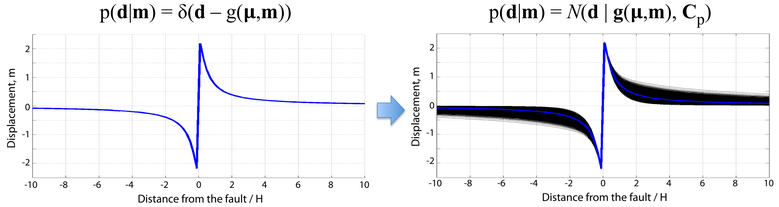

3.2 Calculation of Cp based on the physics of the problem

> A perturbation approach

$\boldsymbol{\delta g} = \mathbf{K}_\mu \cdot \boldsymbol{\delta \ln \mu} \Rightarrow \mathbf{C}_p = \mathbf{K}_\mu \cdot \mathbf{C}_\mu \cdot \mathbf{K}_\mu^T$

Partial derivatives w.r.t. the elastic parameters (sensitivity kernel) | Covariance matrix describing uncertainty in the Earth model parameters

4. Prediction uncertainty due to the earth model $\mathbf{C}_p = \mathbf{K}_\mu \cdot \mathbf{C}_\mu \cdot \mathbf{K}_\mu^T$

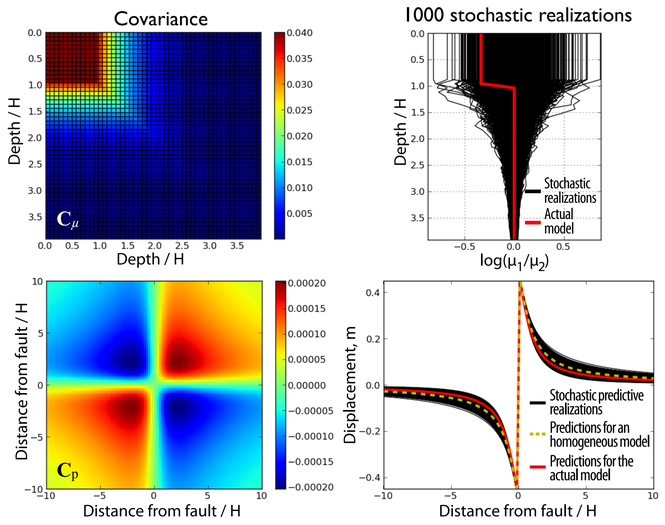

Figure 2. Prediction uncertainty in a two-dimensional quasi-static case. The shear modulus uncertainty is presented on top and the corresponding prediction uncertainty is shown bellow. For each statistical model, we show 1000 stochastic predictions in black assuming a homogeneous half-space.

5. Toy model: Infinite strike-slip fault

> Data generated for a layered half-space (dobs)

> 5mm of uncorrelated observational noise (→$\mathbf{C}_d$)

> Green's functions for an homogeneous half-space (→$\mathbf{C}_p$)

> CATMIP/ALTAR Bayesian sampler (Minson et al., GJI 2013)

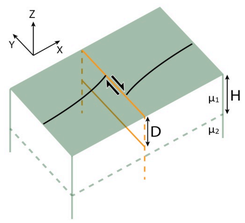

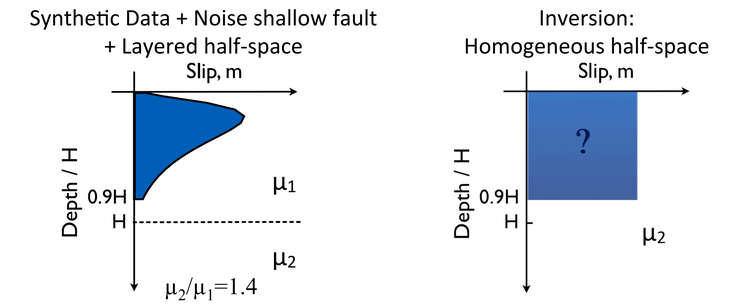

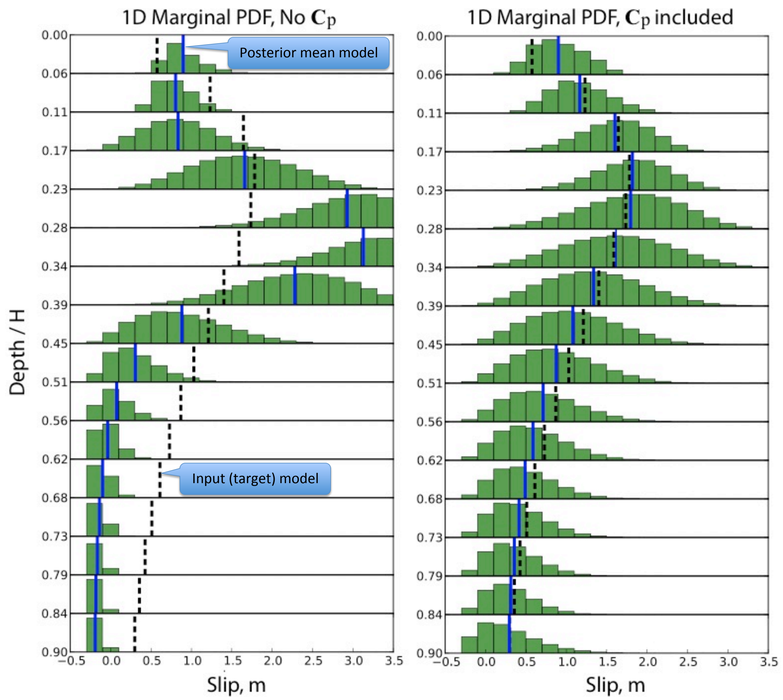

Figure 3. One-dimensional marginal posterior PDFs for each patch as a function of depth. The marginal probability density histograms are shown in green (a) when the prediction uncertainty is neglected and (b) when the prediction uncertainty is taken into account by including Cp in the inversion problem.

6. Why a smaller misfit does not necessarily indicate a better solution

> By neglecting the prediction uncertainty, we tend to overfit the observations using predictions generated for an imperfect Earth model, source geometry, etc.

> Neglecting $\mathbf{C}_p$ can induce significant bias in the solution of the inverse problem.

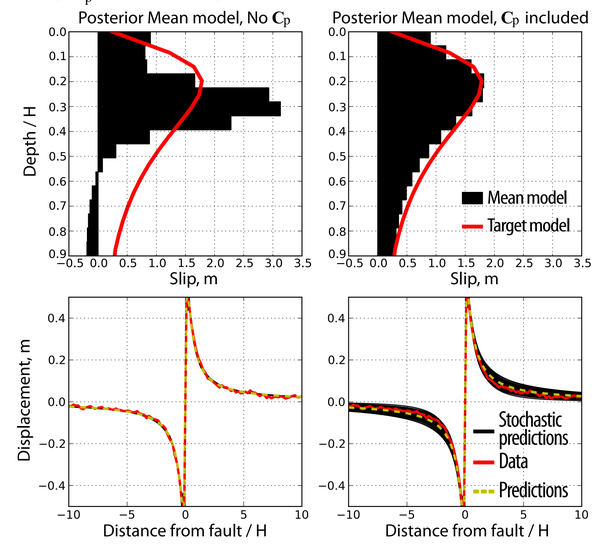

Figure 4. An illustration of overfitting when Cp is neglected. The data is presented in red. The predictions shown in yellow are calculated for the posterior mean models presented in black on top. Black lines correspond to 1000 stochastic realizations drawn from the posterior predictive PDF (i.e., including the variability in $\mathbf{g}(\boldsymbol{\mu},\mathbf{m})$ and the posterior uncertainty in $\mathbf{m}$)

7. Toy model: shallow-dipping thrust fault

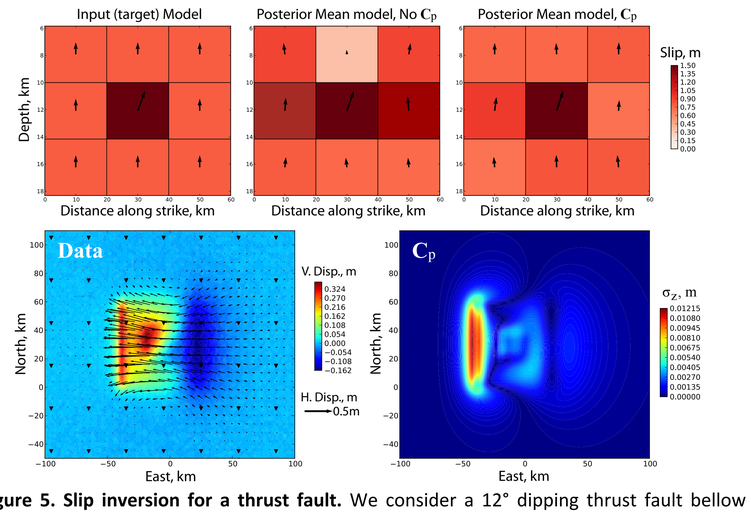

Figure 5. Slip inversion for a thrust fault. We consider a 12° dipping thrust fault bellow a shallow elastic layer of thickness H=5km (μ_2/μ_1=1.4). The inversion is performed assuming an homogenous half-space with or without including Cp. The target and inverted models are shown on top. The Data and the diagonal of Cp are shown bellow.

8. Application to the September 2013 Mw=7.7 Pakistan earthquake

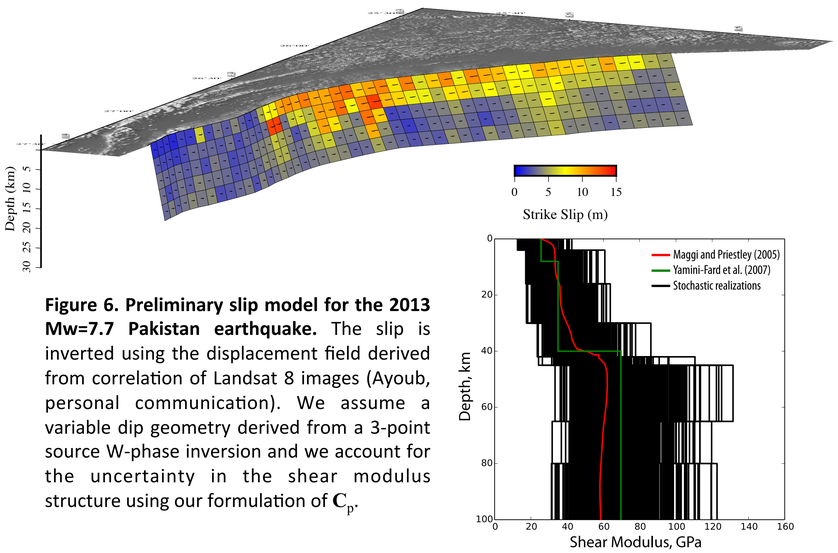

Figure 6. Preliminary slip model for the 2013 Mw=7.7 Pakistan earthquake. The slip is inverted using the displacement field derived from correlation of Landsat 8 images (Ayoub, personal communication). We assume a variable dip geometry derived from a 3-point source W-phase inversion and we account for the uncertainty in the shear modulus structure using our formulation of $\mathbf{C}_p$.